

Resolution Enhancement of Holographic Imaging of Concealed Object using Burg Method

Mujahid Fahmy Al-Azzo

Communications and Electronics Department - Faculty of Engineering - Philadelphia University
P.O.Box: 1 Philadelphia University (19392) – Amman - JORDAN
E-mail : mujaz1@hotmail.com

Abstract

This paper describes a simple and inexpensive technique for the imaging (detection) of concealed object. Burg method is used as a high resolution technique to model the holographic imaging (detecting) problem. Ultrasonic waves are used for imaging a concealed object. The in-line holography is employed. The results demonstrate the enhanced performance capability of the combination of Burg and holographic methods. Also the method showed a much better performance when compared with Fourier transform.

Keywords:

Spectral estimation, ultrasonic waves, signal processing, Burg method, Holographic imaging.

Introduction

The interest in acoustic waves for detection and imaging stems from its properties as highly coherent waves. The ability of ultrasound waves to penetrate many materials that are optically opaque makes them very important for detecting and imaging targets that cannot be imaged by light waves. see [1].

The concealed object is illuminated by acoustic (ultrasound) waves, and the reflected (backscattered) waves are recorded. A transmit/receive ultrasonic transducers are scanning over a synthetic aperture.

The received signal is added electronically to a reference signal, of the same frequency, to generate the in-line holography. The recorded signal is sampled and is known as a hologram. Holography was initiated as an interferometric technique for recording the amplitude and phase of a coherent wave, whether it is electromagnetic or acoustic wave. A recording of this interference pattern is called a hologram, a term coined by Dennis Gabor in 1948, see [2]. It has been applied in the fields of acoustical, and microwave radiations, see [3], [4]. The holographic soundfield imaging technique combines the ultrasonic wave with the holographic interferometry. Holography is one of a two major sources' localization tools, see [5].

The use of holography enables improvement of the signal-to-noise ratio by coherently cumulating the acoustic field on the ultrasonic transducers when scanning the field, see

[6]. The imaging process consists of two steps: the recording of the hologram and the image reconstruction of the object.

The classical (traditional) power spectral estimation methods, also known as non-parametric method, is based on Fourier transformation (FT) of the measured data (observations). This method is computationally efficient, but it suffers from sidelobes, and limited resolution, see [7]. Resolution is a minimum separation between the parts of the object to be resolved. Therefore it is required to look for another method that has much lower sidelobes and better resolution. A modern methods, also known as high resolution methods, contribute in solving the limited resolution and sidelobes problems. A Burg technique is one of these.

The contribution of this paper is to use a high resolution technique (Burg technique) for modeling the ultrasonic holographic imaging problem and use it for imaging (or detecting) a concealed object (concealed rods) by ultrasound waves.

Principle of holographic Imaging

Field analysis at recording axis, see [8]

For simplicity, we start the analysis of the field at the receiving (hologram) axis. The object, under imaging (detection) process, is assumed to have a field distribution $D(p)$. The distribution is caused by reflecting the incident ultrasonic waves on the object. This distribution propagates to the recording axis X where it produces the field distribution $S(x)$, given by:

$$S(x) = \frac{B}{Z_o \lambda} \int_p D(p) \exp(jkr(p, x)) dp \quad (1)$$

This is the paraxial approximation to the Huygens-Fresnel principles. B is a complex constant, k is a propagation constant (wave number), Z_o is the distance between the object and the recording (observation) axis, and r is the distance from a typical point on the object axis to a typical point on the recording axis X . r is given as:

$$r(p, x) = \sqrt{Z_o^2 + (x - p)^2} \quad (2)$$

According to a paraxial approximation, where

$$((x - p)^2 / Z_o^2) \ll 1 \tag{3}$$

(2) is written as:

$$r(p, x) = Z_o + \frac{(x - p)^2}{2Z_o} - \frac{(x - p)^4}{8Z_o^3} + \dots \tag{4}$$

In Fresnel region, r can be approximated by the first two terms of (4), hence

$$r(p, x) = Z_o + \frac{p^2}{2Z_o} + \frac{x^2}{2Z_o} - \frac{px}{Z_o} \tag{5}$$

substituting (5) into (1) yields

$$S(x) = B_1 \exp\left(\frac{jkx^2}{2Z_o}\right) \int D(p) \exp\left(\frac{jkp^2}{2Z_o}\right) \exp\left(\frac{-jkxp}{Z_o}\right) dp$$

(6)

where B_1 is a complex constant resulting from (1) and (5). Analysis of in-line holography can be found in many references, see [2],[9]. The reference wave(a plane wave) for in-line holography can be easily synthesized in an experimental recording system by simply introducing a reference signal, of the same frequency, in the receiver.

Assuming that the synthesized plane-wave reference is $A_r \exp(j\Phi)$ where A_r and Φ are constants. The in-line hologram $h(x)$ is given by

$$h(x) = |S(x) + A_r \exp(j\phi)|^2 = A_r^2 + |S(x)|^2 + A_r \exp(j\phi)S^*(x) + A_r \exp(-j\phi)S(x) \tag{7}$$

where $*$ is a conjugate symbol (operator).

Holographic image reconstruction

An image can be extracted from the recorded hologram $h(x)$ through its multiplication by a phase factor $\exp\left(\frac{-jkx^2}{2Z_o}\right)$ and subsequent use of the classical(FT) method, see[10] or a Burg –based modeling, as in this paper. The phase factor produces an in-focus image from the fourth term of $h(x)$. The first term, A_r^2 , of $h(x)$ is constant and it can be subtracted from the recorded hologram prior to reconstruction, see[10],[6]. The second term produces a defocused autocorrelation function of $D(p)$, and its effect can be reduced by setting A_r few times larger than the maximum of $|S(x)|$.

Principle of Burg Method

The Burg method, see [7], for estimating the AR parameters can be viewed as an order – recursive least-squares lattice method , based on the minimization of the forward and backward errors in linear predictors, with the constraint that the AR parameters satisfy the Levinson-Durbin recursion. To derive the estimator, suppose that we are given the data $S(n)$, $n=0,1,\dots, N-1$, and let us consider the forward and backward linear prediction estimates of order m , given as:

$$\hat{S}(n) = -\sum_{k=1}^m a_m(k)S(n-k) \tag{8}$$

$$\hat{S}(n-m) = -\sum_{k=1}^m a_m^*(k)S(n+k-m) \tag{9}$$

and the corresponding forward and backward errors $f_m(n)$ and $g_m(n)$ defined as $f_m(n) = S(n) - \hat{S}(n)$ and $g_m(n) = S(n-m) - \hat{S}(n-m)$ where $a_m(k)$, $0 \leq k \leq m-1$, $m = 1,2,\dots, p$, are the prediction coefficients. The least square error is

$$\epsilon_m = \sum_{n=m}^{N-1} \left[|f_m(n)|^2 + |g_m(n)|^2 \right] \tag{10}$$

This error is to be minimized by selecting the prediction coefficients, subject to the constraint that the Levinson-Durbin recursion given by

$$a_m(k) = a_{m-1}(k) + K_m a_{m-1}^*(m-k) \quad 1 \leq k \leq m-1 \tag{11}$$

$$1 \leq m \leq p$$

Where $K_m = a_m(m)$ is the m th reflection coefficient in the lattice filter realization of the predictor. When (11) is substituted into the expressions for $f_m(n)$ and $g_m(n)$, the result is the pair of order–recursive equations for the forward and backward prediction errors given by

$$f_m(n) = f_{m-1}(n) + K_m g_{m-1}(n-1), \quad m = 1,2,\dots, p \tag{12}$$

$$g_m(n) = K_m^* f_{m-1}(n) + g_{m-1}(n-1), \quad m = 1,2,\dots, p$$

Now, if we substitute from (12) into (11) and perform the minimization of ϵ_m with respect to the complex –valued reflection coefficient K_m , we obtain the result

$$\hat{K}_m = \frac{-\sum_{n=m}^{N-1} f_{m-1}(n)g_{m-1}^*(n-1)}{\frac{1}{2} \sum_{n=m}^{N-1} \left[|f_{m-1}(n)|^2 + |g_{m-1}(n-1)|^2 \right]} \quad m = 1,2,\dots, p \tag{13}$$

The term in the numerator of (13) is an estimate of the cross correlation between the forward and backward prediction errors. With the normalization factors in the denominator of (13), it is apparent that $|K_m| < 1$, so that the all-pole model obtained from the data is stable. The denominator in (13) is simply the least-squares estimate of the forward and backward errors E_{m-1}^f and E_{m-1}^b , respectively, see [2]. Hence (13) can be expressed as

$$\hat{K}_m = \frac{-\sum_{n=m}^{N-1} f_{m-1}(n)g_{m-1}^*(n-1)}{\frac{1}{2}\left[\hat{E}_{m-1}^f + \hat{E}_{m-1}^b\right]} \quad m=1,2,\dots,p \tag{14}$$

Where $\hat{E}_{m-1}^f + \hat{E}_{m-1}^b$ is an estimate of the total squared error E_m . The denominator term of (14) can be computed in an order-recursive fashion according to the relation, see [7]

$$\hat{E}_m = \left(1 - |\hat{K}_m|^2\right) \hat{E}_{m-1} + |f_{m-1}(m-1)|^2 - |g_{m-1}(m-2)|^2 \tag{15}$$

Where $\hat{E}_m \equiv \hat{E}_m^f + \hat{E}_m^b$ is the total squared error, see [7].

To summarize, the Burg algorithm computes the reflection coefficients in the equivalent lattice structure as specified by (14) and (15), and the Levinson-Durbin algorithm is used to obtain the AR model parameters. From the estimate of the AR parameters, the power spectrum estimate is formed as, see [7]

$$P_{xx}^{BU}(f) = \frac{\hat{E}_p}{\left|1 + \sum_{k=1}^p \hat{a}_p(k) e^{-j2\pi fk}\right|^2} \tag{16}$$

The major advantages of the Burg method for estimating the parameters of the AR model are (1) it results in high frequency resolution, see [7],[11], (2) it yields a stable AR model, see [7],[11], and (3) it is computationally efficient.

Practical Results

A test object consisting of two steel rods of 2.5cm diameter separated by 7.5cm was used to represent the 2-point object. The other experiment parameters were $Z_o = 50cm, \lambda = 0.4cm$ and sampling interval $\Delta x = 1.0cm$. A Styrofoam plate of thickness 3cm was used as a concealing material. The object was illuminated by ultrasonic waves using ultrasonic transmitting transducer. The reflected wave from the object that impinging the receiving transducer is added electronically to a reference signal to form the in-line hologram. The transmit/receive transducers were scanned across the hologram aperture to

sample and record the received signal at uniformly spaced positions Δx . The total number of recorded samples was N.

It is worthwhile to mention that the resolution formula for FT method is given by

$$\sigma = \frac{\lambda Z_o}{a} \tag{17}$$

where a represents half of the aperture length, and given as $a = ((N-1)\Delta x)/2$. (18)

Figure1 shows the result when FT method was used. The greatest two peaks correspond to the power density of the received wave from the rods, while the other peaks represent the sidelobes. The minimum number of samples that was used, to resolve the two rods, was $N = 20$, (aperture length=20 cm). This represents more than twice the minimum number of samples required as given by (17). The degrading effect of the concealing plate is noticeable in the high level of the sidelobes, and the need for large number of samples. The result of using Burg method with $N = 13$ is shown in figure2, where the two peaks correspond to the two rods are clearly defined in spite of the background caused by reflection of the Styrofoam.

To study the problem more deeply, a white noise is added. Figure3 shows the error(in dB) in separation between the two rods as a function of signal to noise ratio (SNR) in the recorded signal. It is clear from the figure that the performance of Burg method for high and low signal to noise ratio is almost the same. Similar results are noticed in figure4 for the difference of intensities of the two peaks that are corresponding to the two rods.

Conclusion

The application of Burg method to the problem of imaging of closely separated parts of concealed object has been demonstrated. it is found that Burg method highly decreases the effect of the concealing material.

References

[1] V. A. Deason, , K. L. Telschow, , and S. M. Watson. Imaging of Acoustic Waves in Sand. *Proc. Of SPIE* 5191: 1-7. 2003.
 [2] U.Schnars, and W. Jueptner, *Digital Holography: Digital Holograms Recording Numerical Reconstruction and Related Techniques*. Berlin- Springer. 2004.
 [3] G.F.Garlick, and J.O. Shelby Detector in ultrasonic holography. *J.Acoustic Soc.Am.* 114: 2995. 2003.
 [4] A.Greve, and D. Morris, Repetitive Radio Reflector Surface Deformation. *IEEE Trans. Antennas & Propagation.* 53: 2123-2126. 2005.
 [5] E.Julliard , S. Pautin, , F. Simon, , and D. Biron,

Acoustic Sources' Localization in Presence of Reverberation. *J.Acoustic Soc.Am.* 118: 1886. 2005.

[6] P. Roux, D. cassereau, , and A. Roux, A High Resolution Algorithm for Wave Number Estimation using Holographic Array Processing. *J.Acoustic Soc.Am.* 115: 1059-1067. 2004.

[7] J.G. Proakis, and D.G. Manolakis. *Digital Signal Processing :Principles, Algorithms, and Applications.* Prentice Hall. 2007

[8] J.W. Goodman *Introduction to Fourier Optics.* Roberts & Company Publisher. 2004.

[9] Saxby, G. eds. 2003. *Practical Holography.* Taylor &

[10] K.H. Sayidmarie , A.P. Anderson, , and J.C. Bennett, Digital In-Line Holographic Techniques for Long Wavelength Imaging, *Proc.IEE.* 129: 211-220. 1982.

[11] R. Bos, S. De Waele, , and P. M.T. Broersen, Autoregressive Spectral Estimation by Application of the Burg Algorithm to Irregularly Francis.

Sampled Data, *IEEE Transaction on Instrumentation and Measurement* 51: 1989-1994 . 2002.

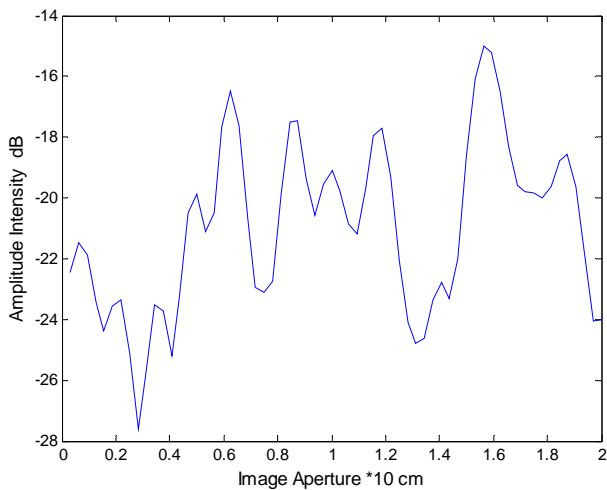


Figure 1-Amplitude intensity of the received power from the two rods using FT method.

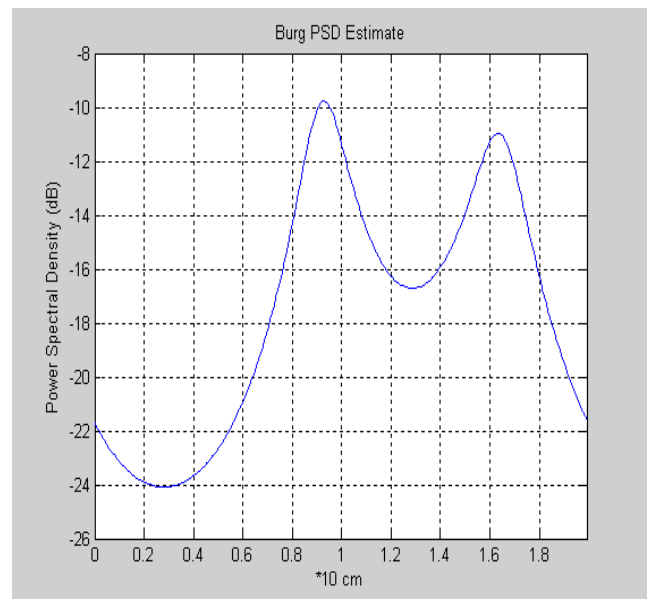


Figure 2- Amplitude intensity of the received power from the two rods using Burg method.

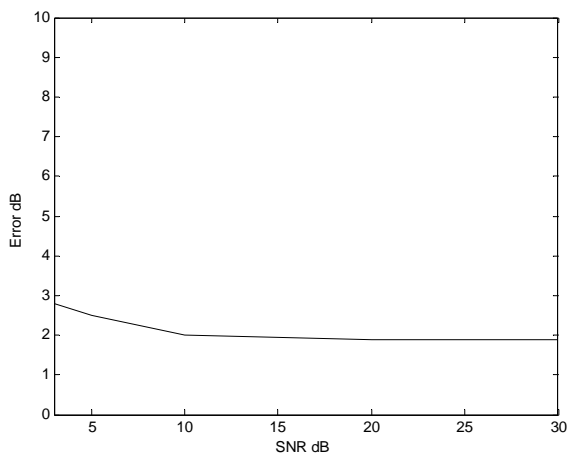


Figure 3 - Error in separation between the two rods as a function of signal to noise ratio, SNR.

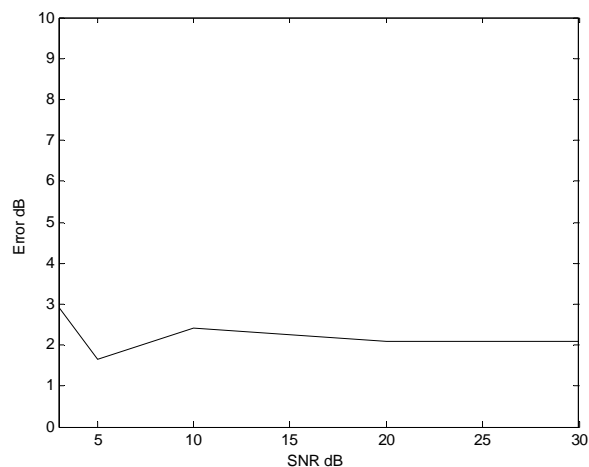


Figure 4 - Error in absolute difference between the two peaks(amplitude) intensity as a function of signal to noise ratio, SNR.